Modeling Dynamic Site Response Using the Overlay Concept

James Kaklamanos[1], Ph.D., A.M. ASCE; Luis Dorfmann[2], Ph.D., P.E.; and Laurie G. Baise[3], Ph.D., M. ASCE

[1] Assistant Professor, Dept. of Civil and Mechanical Engineering, Merrimack College, 315 Turnpike Street, North Andover, MA, 01845, KaklamanosJ@merrimack.edu
[2] Associate Professor, Dept. of Civil and Environmental Engineering, Tufts University, 113 Anderson Hall, Medford, MA, 02155, luis.dorfmann@tufts.edu
[3] Associate Professor, Dept. of Civil and Environmental Engineering, Tufts University, 113 Anderson Hall, Medford, MA, 02155, laurie.baise@tufts.edu

ABSTRACT: Finite element programs allow for an enhancement in the computational capabilities of earthquake site response models. However, many finite element programs involve complicated constitutive models that are difficult for the end user to implement. We present a methodology for modeling earthquake site response within a general finite element framework, using an overlay model to represent nonlinear soil behavior. Using parallel load-carrying elements with varying stiffness and yield stress, the behavior of any given backbone stress-strain relation can be replicated, along with hysteretic unloading-reloading (Masing) behavior. Our finite element modeling methodology makes use of existing conventional elastoplastic material models available in any general finite element program, without requiring the specification of any complicated constitutive models. To represent overlay elements in a finite element model, the user defines a number of finite elements and assigns each of them identical node numbers. The only necessary input parameters are density, elastic constants, and the backbone curve of a stress-strain relation. This paper focuses on the application of one-dimensional total-stress site response, but the framework could be easily extended to model cyclic hardening and softening, three-dimensional wave propagation, and soil-structure interaction.

INTRODUCTION

Site response analyses are used to estimate the ground motion at the surface, as a function of the properties of the soil profile and the "bedrock" ground motion at the base of the soil profile. The equivalent-linear site response model, the most commonly used site response model in engineering practice, was found by Kaklamanos et al. (2013a) to be inaccurate at shear strains of approximately 0.1–0.4%. At larger strains, to model fully nonlinear behavior, the site response calculation should be performed in the time domain, which allows for a more accurate representation of the true cyclic stress-strain path. For many important nonlinear site response applications, such as soil-structure interaction and three-dimensional wave

propagation effects, finite element methods are preferred, especially when complex, non-rectangular geometries are needed.

The purpose of this paper is to present a simple methodology for modeling earthquake site response within a general finite element framework, using the overlay concept set forth by Nelson and Dorfmann (1995). Some nonlinear constitutive models in finite element analyses are difficult to implement and require significant adjustments to existing numerical codes; this paper offers a simple alternative that does not require any modifications to existing finite element programs. Specifically, a number of overlays of simple models are used to achieve a realistic representation of the actual material behavior. As described by Nelson and Dorfmann (1995) and Dorfmann and Nelson (1995), an overlay model uses parallel load-carrying elements with varying stiffness and yield stress, to replicate the behavior of a backbone stress-strain curve. To represent overlay elements in a finite element model, the user defines a number of finite elements and assigns each of them identical node numbers. Because the parallel elements share the same nodal points, the *N* elements have identical strain components: $\epsilon_{ij} = \left(\epsilon_{ij}\right)_1 = \left(\epsilon_{ij}\right)_2 = \cdots = \left(\epsilon_{ij}\right)_N$. The total stress corresponding to a given strain is additively decomposed, and therefore we write: $\sigma_{ij} = (\sigma_{ij})_1 + (\sigma_{ij})_2 + \cdots + (\sigma_{ij})_N$. This simple modeling strategy accounts for hysteretic unloading-reloading behavior, representing Bauschinger's effect (an apparent reduction in yield stress when loads are reversed (Fung 1965)) and Masing behavior (Masing 1926) in a straightforward manner. Under Masing behavior, the stress-strain curve initially follows the backbone curve, and unloading-reloading curves have the same shape as the backbone curve but are enlarged by a factor of two.

When parallel load-carrying elements are defined using the overlay concept in a finite element model, the resulting behavior is consistent with a general class of material models originally conceived by Iwan (1967) and Mroz (1967). Iwan (1967) and Mroz (1967) represented the stress-strain response of a material by using a set of elastoplastic springs connected in parallel. More specifically, each element is composed of a linear spring with shear modulus G_i, and a Coulomb friction element with yield stress τ_{Y_i}, as illustrated in Fig. 1.

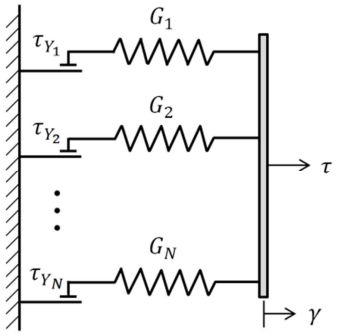

FIG. 1. Schematic of the Iwan (1967) and Mroz (1967) material model composed of elastoplastic springs in parallel.

The Iwan (1967) and Mroz (1967) parallel material model, or modifications thereof, have been applied to soil dynamics in a number of previous studies (e.g., Joyner and

Chen 1975; McKenna and Fenves 2001; Hartzell et al. 2004; Assimaki et al. 2008).

To our knowledge, the geotechnical earthquake engineering literature has not yet seen the application of the overlay concept to modeling site response in a general finite element framework. This paper focuses on the particular application of one-dimensional (1D) site response, but the modeling concept here can be used equally to represent the hysteretic stress-strain behavior of soils under any other dynamic loading condition. In this study, we use the general finite element software Abaqus/Explicit (Dassault Systèmes 2009).

The overlay model presented in this paper has a number of advantages:

1. The model can be implemented with limited geotechnical data (a density profile, shear-wave velocity profile, and modulus-reduction curves).
2. The model can be implemented in nearly any existing finite element code, using standard "off-the-shelf" constitutive models (e.g., elastic – perfectly plastic elements).
3. The basic model is a total-stress representation of nonlinear soil behavior; however, the overlay model can be easily adapted to simulate more complex behavior (such as degradation of the backbone curve and pore pressure generation). The total stress representation may still be used in saturated soils, but excess pore pressures cannot be modeled.
4. This modeling concept can be adapted for two-dimensional (2D) and three-dimensional (3D) site response analyses, offering greater flexibility than the 1D site response programs frequently used.

In this paper, we present the details of our overlay model for earthquake site response within a general finite element framework. First, we explain the mechanics of the overlay model, and how the model may be used to replicate any backbone stress-strain curve, as well as Masing unloading-reloading behavior. Then, we present a newly developed method for determining the shear moduli and yield stresses of the individual overlay elements. Finally, we explain how the overlay model for 1D site response may be implemented in a finite element analysis.

OVERLAY MODELING CONCEPT

When the magnitude of a dynamic load increases, soil experiences a decrease in shear stiffness and an increase in the amount of energy dissipated through hysteretic damping. Nelson and Dorfmann (1995) showed that the overlay modeling concept not only provides the primary stress-strain response, but also accounts for energy dissipation in a simple and natural manner. An illustration of the stress-strain response for the case of $N = 3$ parallel elements is shown in Fig. 2. The total stress-strain curve of the material is given by the addition of the stresses in the individual parallel elements, which are all subject to the same deformation. The stress-strain behavior of an individual element (denoted i) is elastic with shear modulus G_i for shear strains less than γ_i, and becomes perfectly plastic with yield stress τ_{Y_i} for strains exceeding γ_i. The γ_i correspond to the strain values of a backbone stress-strain curve (γ_i, τ_i); the N points of a backbone curve lead to N overlay elements. The stress-strain behavior of the material is defined by a sequence of yield points that occur at increasingly higher stress levels, replicating the behavior of the backbone curve. Specifically, the total

shear stress (τ) for a given shear strain (γ) is represented by the sum of an elastic and plastic component:

$$\tau(\gamma) = \sum_{i=1}^{n} G_i \gamma \; + \; \sum_{i=n+1}^{N} \tau_{Y_i} \,, \tag{1}$$

where n is the number of elements that remain elastic up to strain γ, and N is the total number of elements. For increasing strains, more of the parallel elements are forced to yield, and the load must be carried by a smaller number of elastic elements. As strains increase, the shear stiffness of the material becomes successively smaller. When the final element reaches the elastic limit, the maximum load-carrying capacity of the material is reached, and no further increase in load is possible. The J_2 (von Mises) plasticity criterion is used in the Iwan (1967) and Mroz (1967) material model; although more advanced alternatives are available, the J_2 plasticity criterion is computationally efficient and lends itself well to the overlay model.

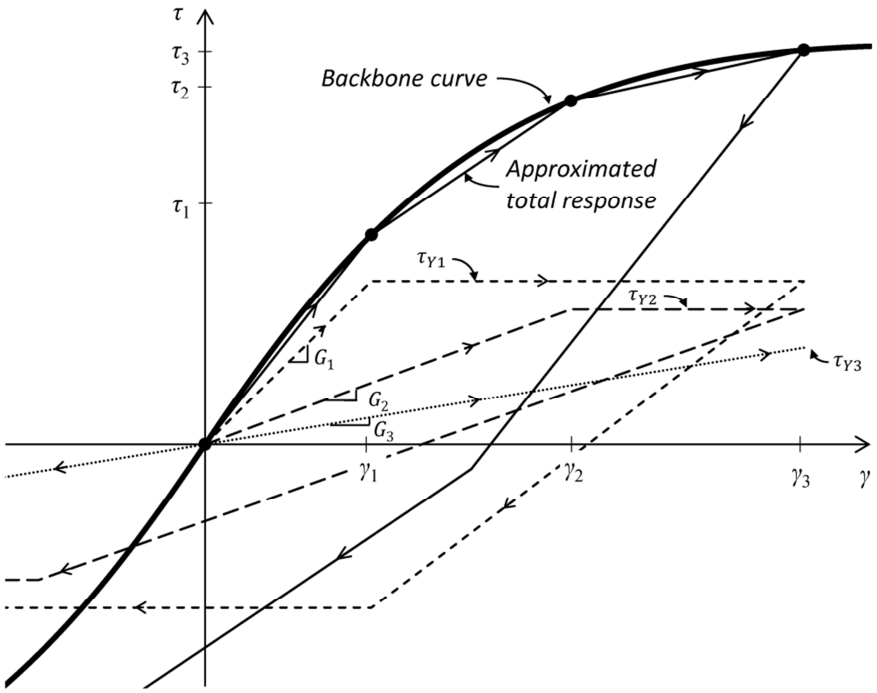

FIG. 2. Stress-strain behavior for N = 3 elastoplastic elements in parallel. Dashed lines indicate the stress-strain behavior of each element, and solid lines indicate the total stress-strain response of the material.

MATERIAL PARAMETERS

Shear moduli and yield stresses

We now describe the material parameters of the overlay model composed of parallel elastoplastic elements. Given a backbone curve $\tau = f(\gamma)$, we must calculate

the shear moduli $(G_1, G_2, \ldots, G_N)$ and yield stresses $(\tau_{Y_1}, \tau_{Y_2}, \ldots, \tau_{Y_N})$ of the N parallel elements for application in a finite element code. We derive a system of equations that directly, for a given backbone curve, gives the magnitude of the shear modulus and yield stress of each individual element. The first step is to linearize the backbone curve into N linear segments, defined by the points (γ_i, τ_i), $i = 1, 2, \ldots, N$. The general stress-strain equation, which represents the multilinear approximation to the backbone curve, can be written as

$$\tau(\gamma) = \begin{cases} (G_1 + G_2 + \cdots + G_N)\gamma & \text{for } 0 \le \gamma \le \gamma_1 \\ \tau_{Y1} + (G_2 + \cdots + G_N)\gamma & \text{for } \gamma_1 \le \gamma \le \gamma_2 \\ \vdots & \\ \tau_{Y1} + \cdots + \tau_{Y(i-1)} + (G_i + \cdots + G_N)\gamma & \text{for } \gamma_{i-1} \le \gamma \le \gamma_i \\ \tau_{Y1} + \cdots + \tau_{Y(i-1)} + \tau_{Yi} + (G_{i+1} + \cdots + G_N)\gamma & \text{for } \gamma_i \le \gamma \le \gamma_{i+1} \\ \vdots & \\ \tau_{Y1} + \cdots + \tau_{Y(N-1)} + G_N\gamma & \text{for } \gamma_{N-1} \le \gamma \le \gamma_N \\ \tau_{Y1} + \cdots + \tau_{Y(N-1)} + \tau_{YN} & \text{for } \gamma \ge \gamma_N \ . \end{cases} \quad (2)$$

Note that each inequality in Eq. 2 is closed, meaning that at the N breakpoints, two possible stress-strain equations are valid: the equations for both the preceding and successive linear segments. This equivalence is possible because the yield stresses τ_{Y_i} are related to the shear moduli G_i by the equation $\tau_{Yi} = G_i\gamma_i$; element i switches from elastic to perfectly plastic at γ_i. Applying Eq. 2 twice at each of the N breakpoints, we obtain a system of $2N$ equations in $2N$ unknowns. Using matrix inversion, we obtain the following general solution for the shear moduli $(G_1, G_2, \ldots, G_N)$ and yield stresses $(\tau_{Y_1}, \tau_{Y_2}, \ldots, \tau_{Y_N})$ for an overlay model composed of N elements:

$$G_1 = \frac{\tau_1}{\gamma_1} - \frac{\tau_1 - \tau_2}{\gamma_1 - \gamma_2} , \quad (3)$$

$$G_i = \frac{\tau_{i-1} - \tau_i}{\gamma_{i-1} - \gamma_i} - \frac{\tau_i - \tau_{i+1}}{\gamma_i - \gamma_{i+1}} , \ \ i = 2, \ldots, N-1 , \quad (4)$$

$$G_N = \frac{\tau_{N-1} - \tau_N}{\gamma_{N-1} - \gamma_N} , \quad (5)$$

$$\tau_{Y1} = \frac{\tau_2\gamma_1 - \tau_1\gamma_2}{\gamma_1 - \gamma_2} , \quad (6)$$

$$\tau_{Yi} = \frac{\tau_{i+1}\gamma_i - \tau_i\gamma_{i+1}}{\gamma_i - \gamma_{i+1}} - \frac{\tau_i\gamma_{i-1} - \tau_{i-1}\gamma_i}{\gamma_{i-1} - \gamma_i} , \ \ i = 2, \ldots, N-1 , \text{ and} \quad (7)$$

$$\tau_{YN} = \tau_N - \frac{\tau_N\gamma_{N-1} - \tau_{N-1}\gamma_N}{\gamma_{N-1} - \gamma_N} . \quad (8)$$

Damping

Nonlinear site response models generally have two types of damping: (a) hysteretic damping, which is associated with energy dissipation within hysteresis loops, and (b) viscous (velocity-proportional) damping, which is associated with dashpots embedded within the material elements. Hysteretic damping (or material damping) is governed by the unloading-reloading rules of the material model; for the overlay model in this paper, Masing behavior (Masing 1926) dictates the area inside the closed hysteresis loops. An equation for the hysteretic damping ratio (ξ) for a backbone curve composed of N linear segments, defined by the points (γ_i, τ_i), $i = 1, 2, \ldots, N$, is

$$\xi(\gamma_a) = \frac{2}{\pi}\left[\frac{\sum_{i=2}^{a}(\tau_i + \tau_{i-1})(\gamma_i - \gamma_{i-1})}{\gamma_a \tau_a} - 1\right] \tag{9}$$

(Ishihara 1996; Kaklamanos 2012). The sum is over a points ($1 \leq a \leq N$), so that the damping ratio can be evaluated for different strain amplitudes, from γ_1 to γ_N. In order to model the hysteretic damping, the user does not need to specify any additional information, because damping is incorporated within the framework of the overlay model itself.

Because there is little hysteretic damping at small strains, many nonlinear site response codes include some level of viscous damping in order to maintain some damping at small strains. In time-domain analyses, Rayleigh damping is the usual mechanism for incorporating viscous damping. The Rayleigh damping coefficients are calibrated to match a particular target damping ratio ξ_{tar} at specified frequencies (Clough and Penzien 2003). Further details on the modeling of viscous damping in the site response overlay model are available in Kaklamanos (2012).

Specification of material parameters in the finite element model

When applying the overlay model in a finite element analysis, the density of each element needs to first be specified. The densities of the individual overlay elements ($\rho_1, \rho_2, \ldots, \rho_N$) are equal to the total material density (ρ) divided by the number of overlay elements: ρ/N. Since the elements are overlain upon one-another, it is necessary to divide by N to ensure that the total density is equal to ρ; otherwise, the total density would be too high. The nonlinear backbone curve $\tau = f(\gamma)$ is then specified using N data points: (γ_1, τ_1), (γ_2, τ_2), …, (γ_N, τ_N). For the N points along the backbone curve, we use Eqs. 3–8 to construct N parallel elements, leading to a shear modulus G_i and yield shear stress τ_{Y_i} for each of the N overlay elements. Sensitivity analyses were performed on the value of N required to adequately represent the material behavior, and we found that the predictions were nearly identical for $N \geq 20$, and there were no significant differences when as low as $N = 10$–15 overlay elements were used.

General finite element codes often require input in terms of Young's modulus (E), Poisson's ratio (ν), and plastic yield stress (σ_Y). Poisson's ratio may be calculated from the P- and S-wave velocities (V_P and V_S), or by assuming some reasonable value (e.g., 0.3). For compatibility, we use the same value of ν for each of the parallel

elements. Using G_i and ν_i, the Young's moduli (E_i) of the elements can then be determined using the standard relation $E_i = 2G_i(1 + \nu_i)$. The plasticity criterion is a J_2 model, and therefore the yield shear stress must be converted to the corresponding von Mises stress. This is accomplished by reducing the von Mises stress equation to $\sigma_{Y_i} = \sqrt{3}\tau_{Y_i}$ for pure shear (the state of stress in a 1D site response analysis).

FINITE ELEMENT ANALYSIS FRAMEWORK

Finite element model

A schematic of the finite element model for 1D site response is shown in Fig. 3. The model consists of a column of reduced-integration 3D brick elements with unit width in the *x*- and *y*-directions, and total height *H* in the *z*-direction, where *H* is the thickness of the geologic profile. In the plane of the page, there is an analogous set of nodes 1 m in the *y*-direction from the nodes shown. The upper layers, representing soil, are modeled by overlays (nonlinear behavior), and the lower layers, representing rock, are modeled by single elements (linear behavior). The loading is applied in the *x*-direction, and all nodes are restrained in the *y*- and *z*-directions. Because each node has one degree of freedom in the horizontal direction, vertically propagating shear waves are modeled. The output from this analysis is the horizontal acceleration (a_x) at the ground surface, as well as shear stress ($\tau = \tau_{xz}$) and shear strain ($\gamma = \gamma_{xz}$) for various elements throughout the soil profile.

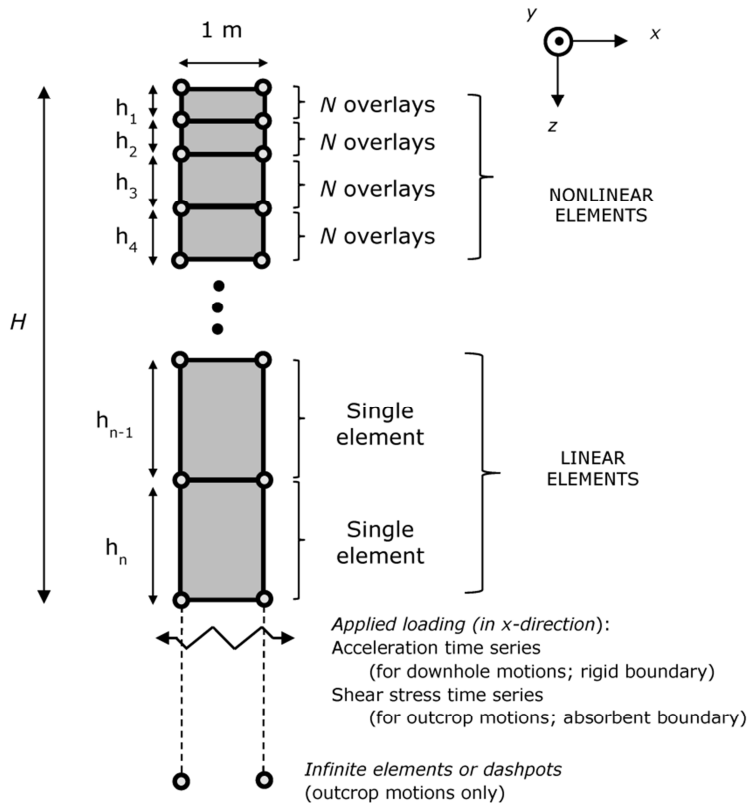

FIG. 3. Schematic of the finite element model for earthquake site response.

In establishing the finite element model, the thicknesses of the elements in the z-direction must be selected in order to consider the transmission of high-frequency energy. In order to transmit shear waves of a specific frequency f, there must be a sufficient number of elements per wavelength in the direction of wave propagation. A general rule of thumb for finite difference and finite element models is to specify 10 grid points per wavelength (Alford et al. 1974). An upper bound on the allowable element thickness h that will allow for the transmission of frequencies up to f_{max} is $h \leq V_S/(10f_{max})$, where V_S is the S-wave velocity of the element. We select f_{max} = 25 Hz for our analyses, because little seismic energy is transmitted at frequencies above this range. This element thickness requirement leads to progressively thinner elements near the top of the soil profile, where V_S is smaller.

Specification of ground motion

The loading and boundary conditions at the bottom of the model are specified in one of two ways, depending on the type of recorded input motion being used (Fig. 4). Input ground motions for site response analyses are obtained either from a downhole recording (also called a "within" motion, some depth below the surface) at a vertical array, or from a surface recording on a rock outcrop (where site effects are assumed to be negligible). As explained in further detail by Kwok et al. (2007) and Kaklamanos (2012), *rigid* boundaries are used when the input motion is taken from a *downhole* recording, and *absorbent* boundaries (representing an elastic base) are used when the input motion is taken from an *outcrop* recording.

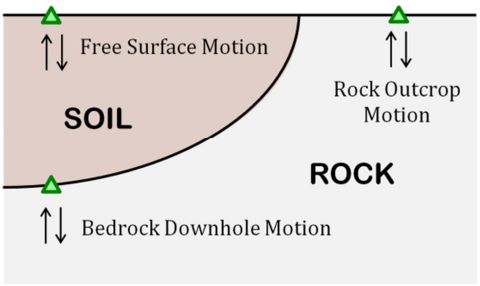

FIG. 4. Illustration of site response terminology, showing the free surface motion (above a soil profile), rock outcrop motion, and bedrock downhole motion.

For the case of a downhole recording being applied to a vertical array site, the input motion may be specified as-is; the acceleration time series is directly specified as a boundary condition at the nodes corresponding to the base of the soil column. This is known as a *rigid* boundary condition; because the motion at the base of the model is completely specified, the base acts as a fixed-displacement boundary and reflects all downward propagating energy back up into the soil column.

On the other hand, when an outcrop recording is applied as an input motion at the base of a soil column, the downgoing waves generated by reflections off the ground surface and the layer interfaces need to be accounted for by the site response model (because the motion itself does not already contain these effects). The loading and boundary conditions are specified in such a manner that downgoing waves are allowed to be transmitted into the underlying bedrock; this is known as an *absorbent*

(or "quiet") boundary condition. We use the methodology of Lysmer and Kuhlemeyer (1969) and Joyner and Chen (1975), in which the acceleration time series is expressed as a shear stress time series at the base of the model:

$$\tau(t) = \rho_r V_{S_r} v_{outcrop}(t) \,, \tag{10}$$

where $\tau(t)$ is the shear stress time series applied at the boundary, ρ_r is the density of the underlying material (basement rock), V_{S_r} is the shear-wave velocity of the basement rock, and $v_{outcrop}(t)$ is the velocity time series of the input ground motion, obtained from a rock outcrop recording at the ground surface. In a general finite element model, the absorbent boundary scheme can be applied in one of two ways, through the use of (a) infinite elements, or (b) viscous dashpots. Details are described further in Kaklamanos (2012).

SUMMARY

Our overlay model for earthquake site response has a number of advantages for its usage in engineering research and practice: the model requires basic geotechnical data, can be implemented in nearly any existing finite element code, and can be easily adapted to model more complex behavior (such as cyclic hardening and softening, soil-structure interaction, and two- and three-dimensional site response), without the specification of any complicated constitutive models. The reader is referred to Kaklamanos (2012) for a detailed validation and verification of the overlay model using a station in the Kiban-Kyoshin network (KiK-net) of downhole arrays in Japan, as well as an extension of the overlay model to simulate cyclic hardening and softening. Kaklamanos (2012) and Kaklamanos (2013b–c) also provide validations using a greater number of KiK-net sites and ground motions, as well as comparisons to other site response models. The overlay model displays an improvement in prediction accuracy over other standard site response models. Although this paper has implemented the overlay model in the context of 1D site response, the modeling strategy of parallel plasticity is extremely flexible, and allows for the representation of hysteretic stress-strain behavior in a broad range of dynamic loading conditions.

ACKNOWLEDGMENTS

This research was supported under National Science Foundation (NSF) Grant No. 1000210; we gratefully acknowledge this support. Eric Thompson (San Diego State University) offered important contributions, and David M. Boore (U.S. Geological Survey) provided helpful feedback on an earlier version of this manuscript. We also thank Dr. Adrian Rodriguez-Marek (Virginia Tech) for making the finite element modeling work of his former student, Surendran Balendra, available to us.

REFERENCES

Alford, R.M., Kelley, K.R., and Boore, D.M. (1974). "Accuracy of finite difference modeling of the acoustic wave equation." *Geophysics*, Vol. 39: 834–842.

Assimaki, D., Li, W., Steidl, J., and Schmedes, J. (2008). "Quantifying nonlinearity

susceptibility via site response modeling uncertainty at three sites in the Los Angeles basin." *Bull. Seism. Soc. Am.*, Vol. 98: 2364–2390.

Clough, G.W. and Penzien, J. (2003). *Dynamics of structures*, 2nd ed. revised, Computers and Structures, Inc., Berkeley, Calif.: 739 pp.

Dassault Systèmes (2009). *Abaqus 6.9-2*, Providence, R.I.

Dorfmann, A. and Nelson, R.B. (1995). "Inelastic response of column/girder connections to seismic loads using parallel plasticity." *Numerical methods in structural mechanics*, J.W. Ju, ed. (AMD-Vol. 204), ASME: 13–29.

Fung, Y.C. (1965). *Foundations of solid mechanics*, Prentice Hall, Englewood Cliffs, N.J.: 525 pp.

Hartzell, S., Bonilla, L.F., and Williams, R.A. (2004). "Prediction of nonlinear soil effects." *Bull. Seism. Soc. Am.*, Vol. 94: 1609–1629.

Ishihara, K. (1996). *Soil behavior in earthquake geotechnics*, Oxford University Press, New York: 350 pp.

Iwan, W.D. (1967). "On a class of models for the yielding behavior of continuous and composite systems." *J. Appl. Mech.*, Vol. 34: 612–617.

Joyner, W.B. and Chen, A.T.F. (1975). "Calculation of nonlinear ground response in earthquakes." *Bull. Seism. Soc. Am.*, Vol. 65: 1315–1336.

Kaklamanos, J. (2012). *Quantifying uncertainty in earthquake site response models using the KiK-net database*, Ph.D. Dissertation, Tufts University, Medford, Mass.: 300 pp.

Kaklamanos, J., Bradley, B.A., Thompson, E.M., and Baise, L.G. (2013a). "Critical parameters affecting bias and variability in site response analyses using KiK-net downhole array data." *Bull. Seism. Soc. Am.*, Vol. 103: 1733–1749.

Kaklamanos, J., Dorfmann, L., and Baise, L.G. (2013b). "Quantification of uncertainty in nonlinear soil models at a representative seismic array." *11th International Conference on Structural Safety and Reliability (ICOSSAR 2013)*, New York City, New York, 16–20 June 2013.

Kaklamanos, J., Baise, L.G., Thompson, E.M., and Dorfmann, L. (2013c). "Modeling nonlinear 1D site response at six KiK-net validation sites." *2013 Annual Meeting of the Seismological Society of America (SSA),* Salt Lake City, Utah, 17–19 April 2013 (abstract printed in *Seismol. Res. Lett.*, Vol. 84: 317)

Kwok, A. O. L., Stewart, J.P., Hashash, Y.M.A., Matasovic, N., Pyke, R., Wang, Z., and Yang, Z. (2007). "Use of exact solutions of wave propagation problems to guide implementation of nonlinear, time-domain ground response analysis routines." *J. Geotech. Geoenv. Eng*, Vol. 133: 1385–1398.

Lysmer, J. and Kuhlemeyer, R.L. (1969). "Finite dynamic model for infinite media." *J. Eng. Mech. Div.*, Vol. 95: 859–877.

Masing, G. (1926). "Eigenspannungen and verfertigung beim messing." *Proc. 2nd International Congress on Applied Mechanics*, Zurich, Switzerland.

McKenna, F. and Fenves, G.L. (2001). *The OpenSees Command Language Manual, Version 1.2,* Pacific Earthquake Engineering Research Center, Berkeley, Calif.

Mroz, Z. (1967). "On the description of anisotropic workhardening." *J. Mech. Phys. Solid.*, Vol. 15: 163–175.

Nelson, R.B. and Dorfmann A. (1995). "Parallel elasto-plastic models of inelastic material behavior." *J. Eng. Mech.*, Vol. 121: 1089–1097.